Inter*net* Electronic Journal*

Nanociencia et Moletrónica

Julio 2010, Vol. 8, N°1, pp. 1445 -1458

Micro-structural changes in the amorphous Fe-based alloy 2605S3A prior to crystallization

Part 1: Differential scanning calorimetry, heating treatment, X-ray diffraction and Vickers micro-hardness

A. López-Morales[1], A. Cabral-Prieto[2], F. García-Santibáñez[1], J. Ramírez[2], J. López-Monroy[2]

[1] Laboratorio de Física de Materiales, Facultad de Ciencias, Universidad Autónoma del Estado de México. El Cerillo Piedras Blancas, Toluca, Estado de México, **México**
[2] Instituto Nacional de Investigaciones Nucleares (ININ), Ocoyoacac, Estado de México, **México**.

recibido: 16.10.09 revisado: 15.04.10 publicado: 31.07.10

Citation of the article;
A. López-Morales, A. Cabral-Prieto, F. García-Santibáñez1, J. Ramírez, J. López-Monroy. Simulación del Micro-structural changes in the amorphous Fe-based alloy 2605S3A prior to crystallization, Part 1: Differential scanning calorimetry, heating treatment, X-ray diffraction and Vickers micro-hardness Internet Electron J. Nanoc. Moletrón, 2010, Vol. 8, N°1, pp 1445-1458

Micro-structural changes in the amorphous Fe-based alloy 2605S3A prior to crystallization

Part 1. Differential scanning calorimetry, heating treatment, X-ray diffraction and Vickers micro-hardness

A. López-Morales[1], A. Cabral-Prieto[2], F. García-Santibáñez[1], J. Ramírez[2], J. López-Monroy[2]

[1] Laboratorio de Física de Materiales, Facultad de Ciencias, Universidad Autónoma del Estado de México. El Cerillo Piedras Blancas, Toluca, Estado de México, México
[2] Instituto Nacional de Investigaciones Nucleares (ININ), Ocoyoacac, Estado de México, **México**.

recibido: 16.10.09 revisado: 15.04.10 publicado: 31.07.10

Internet Electron. J. Nanoc. Moletrón., 2010, Vol.8, N° 1, pp 1445-1458

Abstract

Clusters of 24 and 32 mono-vacancies in the amorphous and crystalline states of the 2605S3A alloy, respectively, having 0.44 nm mean radii and a mean relative concentration of clusters of $C = 1.68x10^{-8}$ atoms^{-1} between these states were measured by the positron annihilation process. Slight variations of size and of the concentration of these clusters were the source of micro-structural changes in the alloy as reflected in its mechanical properties, magnetic properties and phase transitions. These results are analyzed in terms of the micro-structural changes occurring in the alloy using differential scanning calorimetry (DSC) and X-ray diffraction (XRD). Moreover, nanometric changes in the sample are detected by using Mössbauer spectroscopy and Vickers micro-hardness measurements.

Keywords: amorphous alloy, thermal treatment, magnetic properties, nanocrystalline material.

Resumen

Cúmulos de 24 y 32 monovacancias en los estados amorfo y cristalino, de la aleación 2605S3A. Ellos tienen radios medios de 0.44nm y una concentración media relativa de cúmulos de $C = 1.68x10^{-8}$ átomos^{-1} para ambos estados amorfo y cristalino, que fueron medidos por el proceso de aniquilación de positrones. Las ligeras variaciones del tamaño y la concentración de estos cúmulos fueron la fuente de cambios microestructurales en la aleación, como se reflejaron en sus propiedades mecánicas y magnéticas y en las transiciones de fase. Estos resultados son analizados en términos de los cambios microestructurales que ocurrieron en la aleación usando DSC y XRD. Además, los cambios nanométricos en las muestras fueron detectados usando Espectroscopia Mössbauer y medidas de microdureza Vickers.

Descriptores: aleación amorfa, tratamiento térmico, propiedades magnéticas, material nanocristalino

1. Introduction

Since the first developments on inter-metallic compounds in 1946 [1], several scientific and technological interests have remained ever since. One of these interests is connected with the production of amorphous alloys with soft magnetic properties, by which the chemical composition of the alloys has thoroughly been modified and investigated. There have emerged from this effort not only several techniques to produce them but also a great variety of alloys with different elemental compositions and magnetic properties. The technological applications of these amorphous alloys have been restricted to low-working temperatures because of their mechanical properties, which become brittle in the crystalline state. This mechanical handicap appears either in thin sheets or bulk amorphous alloys, and whether this handicap can be subdued is a matter of continuous research [2, 3]. Particularly, the ductility of the Fe-based amorphous alloys slowly decreases while being transformed from the amorphous to the crystalline state [3]. Such a loss of ductility is generally accepted to be due to the presence of different crystalline phases from pure Fe in the crystalline state [4]. Another source contributing to such a loss of ductility is the presence of crystalline defects, which may vary from micro- to nanometric sizes, or in concentration prior to or throughout the phase transitions. Such variations in size and/or concentration of defects have been reported to produce other property changes in the alloy, like changes in the magnetic properties [5]. Thus, the brittleness problem of these Fe-based amorphous alloys greatly depends on the elemental nature of the alloy, the presence of crystalline phases other than pure Fe and on mass and/or volumetric defects and their concentration, among other sources.

Thus, in the present paper the Fe-based amorphous alloy 26053SA was thermally treated from 325 to 810K, where the mechanical properties were studied by measuring the Vickers micro-hardness number, H_V. The corresponding micro-structural changes occurring in the alloy were studied by using Mössbauer spectroscopy (MS) [6], X-Ray Diffraction (XRD) and DSC.

2. Experimental

The Fe-based amorphous alloy 2605S3A was obtained from Metglass Inc. Co., USA as a gift from J. Jordan and Dr. Hasegawa. The elemental composition analysis of the alloy was carried out with the Proton Induced X-ray Emission (PIXE) technique [7], where accelerated protons of 3 MeV were directed to an untreated sample coming from the Tandem accelerator at the Nuclear Center of México; the X-rays emitted from the sample were detected by using the Si-Li detector, model 3010, from Kevex-X-Ray.

Additional samples were cut from the original sheet of the dimensions as required by the experiment and then were thermally treated from 325 to 810K by using the small furnace, model VF-1000 from ASA, connected to a temperature controller, model S8-VF from ASA. The furnace was kept connected to a vacuum system with $4x10^{-7}$ torr. The maximum temperature reached in each thermal treatment was maintained for 20 minutes before cooling the sample. A series of experiments was carried out by using a constant heating rate (CHR) of 3 ± 0.12 K/min. Another series of experiments was carried out by employing variable heating rates (VHRs) ranging from 1.8 to 6.1 K/min. The cooling rates on both series were relatively low and of exponential type. The glass and crystalline phase

transitions were measured with the Differential Scanning Calorimeter SDT, model Q600 from TA Instruments with heating rates of 3 and 5K/min.

The Vickers micro-hardness number H_V was measured by using the Buehler 5101Micromet apparatus with a load of 0.4903 N/10 s. Three small samples were used for this purpose and seven indentations were made on each side of the samples. Thus, the reported data is the average value of 42 indentations. Some of the samples used in the H_v measurements were replaced by new ones after the 723K treatment because of the brittleness problem of the alloy.

The XRD patterns of the treated samples were registered with the D5000 diffractometer coupled to a CuKα X-Ray source from Siemens.

The Mössbauer spectra were recorded by using a conventional constant acceleration Mössbauer spectrometer with a ^{57}Co/Rh radioactive source. The isomer shift (δ) of the resulting spectra is referred to that of metallic α-Fe, and the spectra were analyzed by using the Normos program [8].

For all the preceding measurements, foils of 2 cm long x 2 cm wide were used. For the DSC measurements the samples were cut, as required by the instrument.

While the samples heat-treated with the CHR of 3K/minute were used for H_V measurements, the samples heat-treated with VHRs were used for the XRD and MS ones.

3. Results and discussion

3.1 PIXE

The PIXE spectrum showed characteristic peaks of Fe, Cr, Mn and Si. Atomic mass with $Z \leq 12$, however, cannot be detected by this technique. The quantitative analysis of the PIXE spectrum was carried out by using the GUPIX program [7] giving the following weight percent results: $Fe_{95.30}Cr_{2.46}Mn_{0.14}Si_{0.90}$.

3.2 DSC and HRs

Two exothermic processes were detected by the DSC measurements as shown in Fig. 1. When different heating rates are used (9), these processes appear at different temperatures For instance, when the CHR of 3K/min. was used, these processes appeared at 779 and 795K, but when a CHR of 5K/min. was used, these processes appeared at 785 and 802K. The full width at half maximum of these exothermic peaks was of 8K. Therefore, there was a small temperature shift of 6 and 7 K between the first and second processes while using the CHR of 3 and 5 K/min., respectively. While the first process is usually associated with the glass transition or the first crystallization process, the second one is associated with the second crystallization process of the alloy.

Hence, due to the fact that samples for the Mössbauer and XRD measurements were heated by using VHRs, ranging between 1.8 and 6.1 k/min., and the samples for the H_V measurements were heated by using the CHR of 3K/min., some of the results among these techniques might not be fully correlated due to small temperature shifts. Such discrepancies, however, being small do not modify the main trend of the present results.

On the other hand, Fig. 2 shows a typical heating and cooling process of a sample, consisting of three steps: (1) the heating process of the sample up to the desired temperature by using either the CHR or a VHR, (2) the selected temperature of each treatment was kept constant for 20 min., and (3) the cooling process of the samples was

multi-exponential and relatively slow for all heat treatments. The cooling rates ranged between 1 and 4K/min. The high cooling rates appeared while cooling the samples from 772 and 810K. Below this temperature interval, low cooling rates set in on the heater.

3.3 H_V

After each thermal treatment, the Vickers micro-hardness of the sample was measured, as already described in the experimental section, and the results are

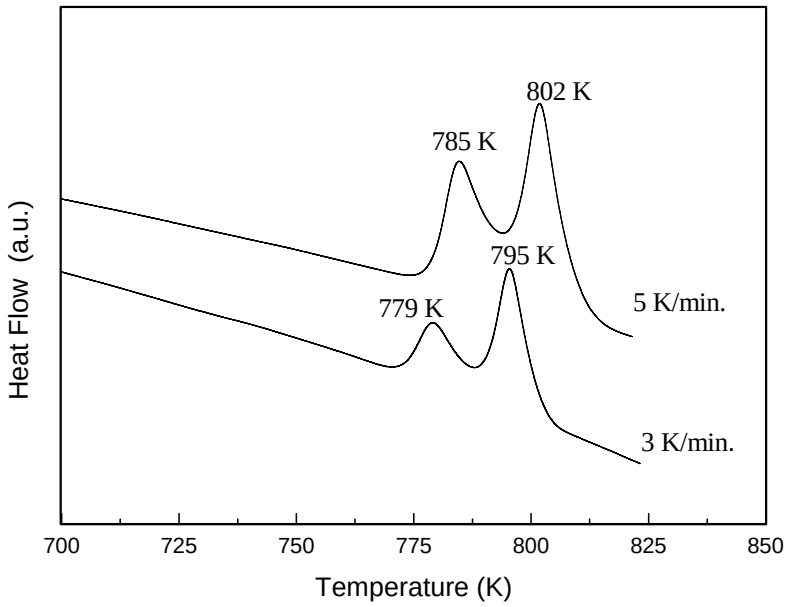

Fig.1. DSC curves of the amorphous 2605S3A alloy at two heating rates.

shown in Fig. 3. Three characteristic features can be observed from Fig. 3: (1) The Vickers number practically remains constant between 300 and 589K with only a very slight decrease and having an average value of $H_V = 9.18 \pm 0.08$ GPa. The alloy

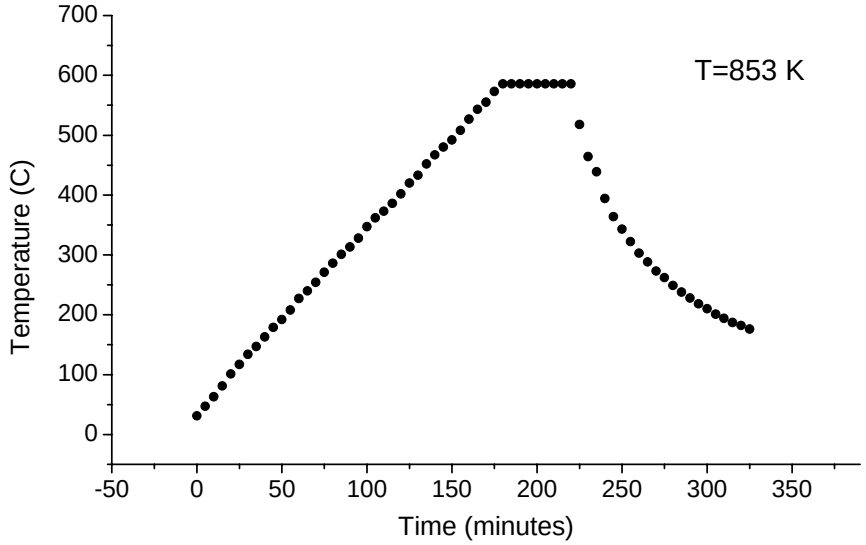

Fig.2. Typical heating and cooling treatment subjected to the alloy at CHR of 3 K/min.

preserves its ductility after these thermal treatments; (2) After treating the sample between 634 and 699K, the measured Vickers number increased somewhat and remained constant with an average value of H_v = 9.49 ± 0.05 GPa; after treating the alloy at 699K, its ductility was very poor even when it remained in its amorphous state. (3) The next feature of the H_V data, measured between 725 and 810K is characterized by having the highest values of the Vickers number with an average value of H_V. = 10.8 ± 0.28 GPa. At the end of each of these latter thermal treatments, the alloy was completely brittle. However, a significant decrease of the Vickers number was measured after the treatment at 772K. This decrease on H_V occurred at 7K prior to the temperature peak of the first exothermal process as detected by the DSC measurements (Fig. 1). This minimum on the H_V values must therefore be associated with the start of the first phase transition.

Generally speaking, the variations of H_V against temperature (T) might be discussed by using the Hall-Petch relation [10]

$$H_v = \sigma_i + k_f d^{-\frac{1}{2}}, \quad (1)$$

which relates the Vickers number and grain size *d*. Here σ_i represent the deformation constant of the material and k_f the minimum energy to move a dislocation. Eq. (1) is usually applied to the crystalline state of metals, where the presence of grains is a common feature. If Eq. (1) were applied to the amorphous state of the alloy, k_f would represent the energy to move or modify a region of low mass density in the alloy and *d* the size of a region of high mass density, i. e., the amorphous grain [10,11]. Thus,

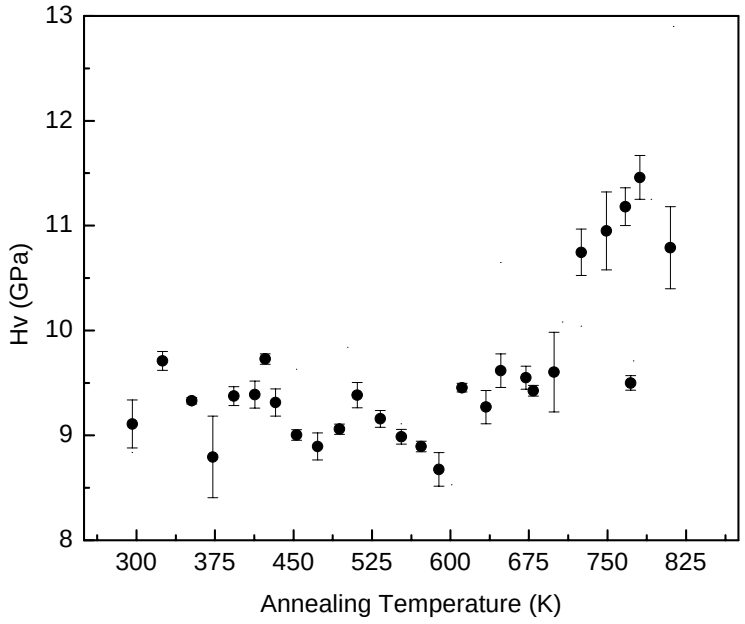

Fig.3. Vickers micro-hardness numbers variations from the amorphous 2605S3A alloy with different annealing temperatures.

the pronounced decrease of H_V at 772K could be associated with the variation of the amorphous grain size just before the first crystallization process. In particular, the decrease of H_V at 772K would suggest an increase of these grains [10,11] or grain formation.

3.4 XRD

Some of the micro-structural changes of the thermally treated alloy can also be studied by their XRD patterns, which are shown in Figs. 4 and 5, where the number preceding TC (thermal constant) or TV (thermal variable) indicates the number of thermal treatment. Fig. 4 shows four special XRD patterns from which the start of the crystallization process can be observed. As can be seen from Fig. 4, after treating the alloy sample at 749K, it still remained in its amorphous state, but after treating it at 766 and at 775K a small peak began to emerge at about 45^0, suggesting the start of the crystallization process. As already described, the decrease of H_V at 772K must, therefore, be associated with the first crystallization process and possibly with the grain formation in the crystalline state. One should also notice that there are no significant differences between thermal treatments while CHR or VHRs is used at this stage of the analysis.

On the other hand, Fig. 5 shows the XRD patterns of the crystallized samples by using either CHR or VHRs. The relevance of Fig. 5 is that the XRD patterns of a sample treated at 781 and then at 810K in its 24^{th} and 25^{th} treatments, by using the CHR of 3k/min., are, to a certain degree, due to pure Fe. This is especially true for the 810K pattern. On the other hand, the XRD pattern, recorded after treating a sample in a single thermal treatment at 813K by using a VHR between 3 and 5k/min other crystalline phases than pure Fe are present. These additional phases can possibly be discarded for a sample treated nine times from 325 to 792K by using VHRs between 2 and 6.1K. These results

then suggest that crystalline phases, different from pure Fe, can be inhibited by subjecting a sample to many thermal treatments below the transition temperatures, T_g and T_x. How these inhibition processes affect the mechanical properties of the alloy is now a subject of careful study.

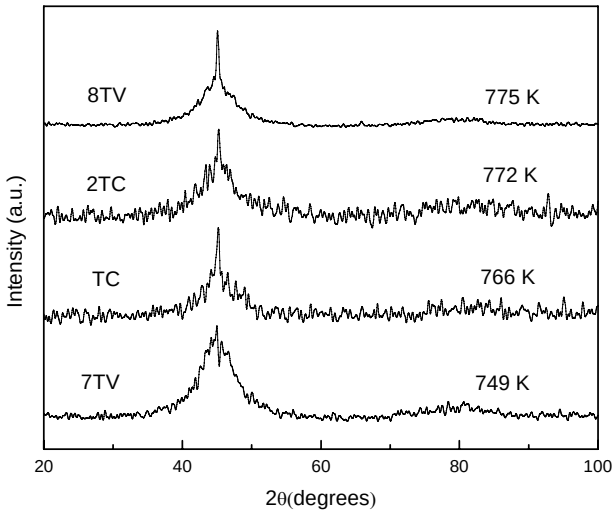

Fig.4. XRD patterns of the amorphous 2605S3A alloy after some heat treatments as indicated in the text.

3.5 MS

Figure 6 shows some Mössbauer spectra of the thermally treated alloy. A typical Mössbauer spectrum of these amorphous alloys consists of a broadened magnetic sextet, in which the relative peak intensities deviate from a randomly magnetically oriented sample (Fig. 6). For the general case, where the direction of B_{hf} at the nucleus is randomly oriented, the relative peak-area ratios are: 3:α:1:1:α:3 with α = 2 [6].

The peak intensity variations of the Mössbauer spectra, shown in Fig. 6, were evaluated in order to determine the magnetic reorientation in the sample by using the following formula [6]

$$\alpha = \frac{4\sin^2(\theta)}{1+\cos^2(\theta)}, \qquad (2)$$

where α represents the peaks-area ratio between peak-area 2 to peak-area 3 and/or peak-area 5 to peak-area 4 of the Mössbauer sextet and θ is the angle between the emitted 14.4 KeV gamma ray direction and that of the hyperfine magnetic field (B_{hf}) at the iron nucleus (6). These parameters are given in Table 1. Before analyzing the data of Table 1, it can be observed that the alloy remains in its amorphous state after the 775K treatment. Crystalline material was not detected in this case as it was by

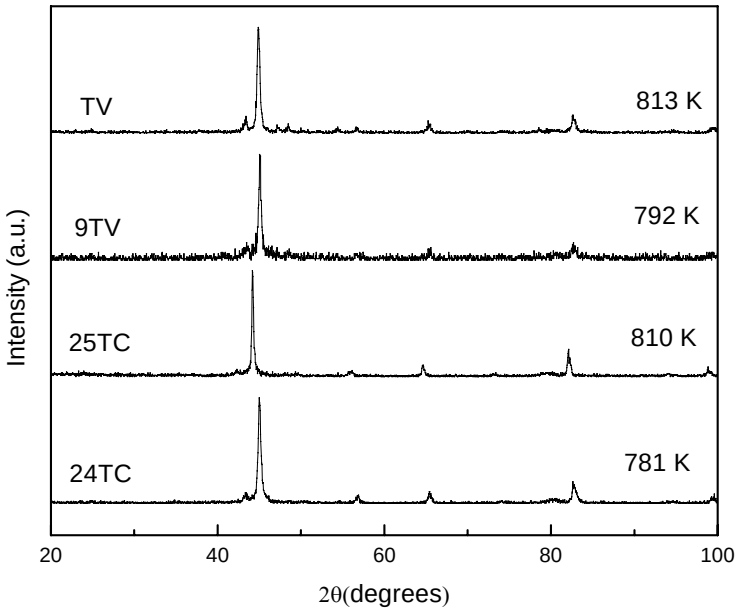

Fig.5. XRD patterns of the amorphous 2605S3A alloy after some of the heat treatments as indicated in the text.

the corresponding XRD pattern (Fig 4). The explanation for this is that the Mössbauer sample was generally subject to HRs higher than 3K/min., as already stated in the experimental section. Despite this, other important micro-structural changes occurred in the alloy after the 772 and 775K treatments, i. e., near the first phase transition. It is indeed interesting to note that after the 772K treatment, the Mössbauer spectrum of the alloy was characteristic of the amorphous material but magnetically reoriented; the intensities of peaks 2 and 5 were minima after these thermal treatments. Hence, besides the phase change, detected by XRD measurements, and the minimum of H_V measured after the 772K treatment, a magnetic reorientation in the sample also took place. On the other hand, the Mössbauer spectrum of the sample treated at 792K corresponds to a crystallized sample where more than one sextet is present, thus suggesting the presence of other crystalline phases than pure Fe.

The Mössbauer results of a sample that is thermally treated many times before its crystallization will be presented in a different paper in which the inhibition process of additional crystalline phases different from pure Fe will be further analyzed.

On the other hand, it is to be noticed from Fig. 6 that at any spectrum there appears signs of nano-crystalline material. If it were present, part of the Mössbauer magnetic spectrum would collapse into single or double lines. This is not the case in any one of the present spectra shown in Fig. 6.

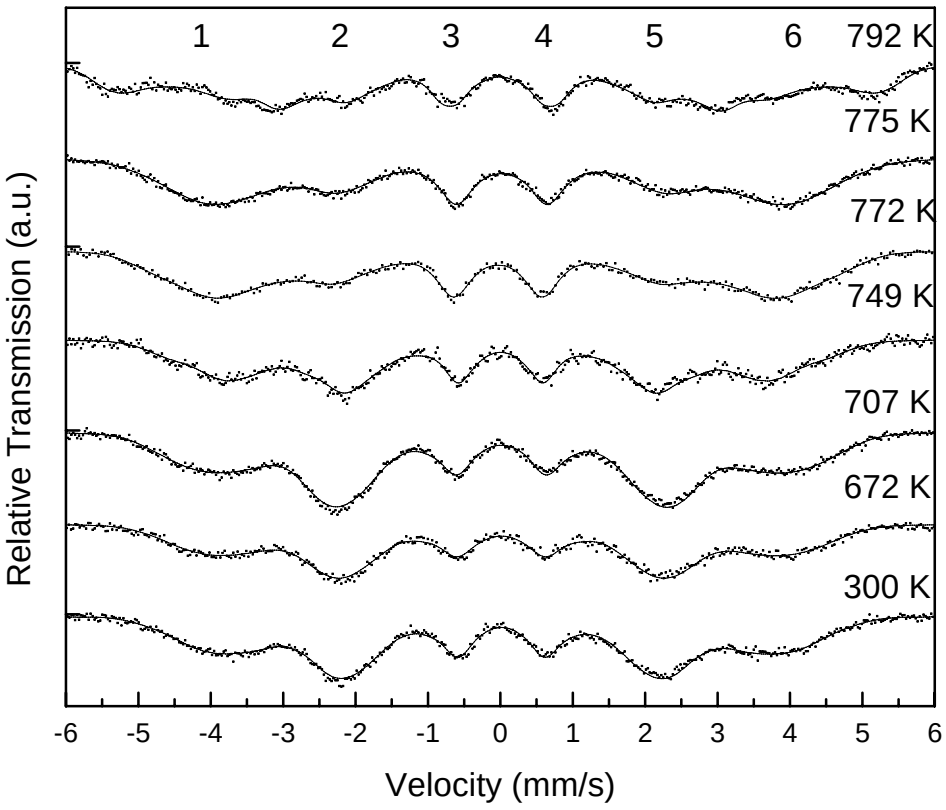

Fig.6. Mössbauer spectra of the amorphous and crystalline 2605S3A alloy annealed at different temperatures.

Passing by the absence of super-paramagnetism in the present alloy without any further comment and according to the fitting analysis of the Mössbauer spectra of the amorphous alloy only, an average value of α = 2.9 was obtained between 300 and 648K (Table 1) giving $\theta = 66^0$ from Eq. (2). A value of α = 4 was obtained from the recorded Mössbauer spectrum of the alloy after treating it at 672K and now $\theta = 90^0$, i. e., the direction of B_{hf} with respect to the direction of the gamma rays of 14.4 keV is fully perpendicular. On the other hand, a minimum value of α = 1.29 was obtained from the recorded Mössbauer spectrum after treating the alloy at 772K, and $\theta = 44^0$ results (see Table 1).

Indeed, after treating the alloy at 749K, the lowest value of B_{hf} = 22.59 T was obtained. This minimum was measured 30K below the temperature of the first crystallization process, suggesting that the Fe-Fe distances may be the largest [10]. This result should be connected with both free volume and electronic changes

Table 1**.** Mössbauer peak-area ratios α and the corresponding angles θ calculated from Eq. (2)

T (K)	α	θ (Degrees)
300	3.02	68.10
453	2.89	66.39
502	3.07	68.73
553	2.97	67.45
601	2.98	67.53
648	2.64	63.07
672	4.00	90.00
704	2.42	60.26
707	3.54	75.74
749	2.25	58.08
766	1.59	48.96
767	2.09	55.94
772	1.29	44.26
775	1.40	46.11

around the Fe atoms. Furthermore, a neat increment of B_{hf} was measured between 766 and 775K where the first crystallization process should start, with B_{hf} = 24.01 T (Table 2). This increment should also be associated with the shortening of the Fe-Fe distances and change of electronic density around the Fe atoms because of the phase transition [10]. The changes of electron density can be studied by analyzing

Table 2. Mössbauer parameters of the Fe-based alloy 2605S3A, after being treated at different temperatures.

T (K)	B_{hf} ($\pm$ 0.07) (T)	δ ($\pm$ 0.03) (mm/s)	Δ_Q**($\pm$ 0.01)** (mm/s)
300	23.05	0.109	-0.031
502	23.14	0.094	-0.029
648	23.80	0.111	-0.025
672	23.43	0.123	-0.028
749	22.59	0.094	-0.041
766	24.01	0.070	-0.015
772	23.88	0.069	-0.017
775	24.30	0.114	-0.030
792	25.75	0.088	-0.034

the isomer shift (δ), which is directly related to the S-type electron density inside the Fe nucleus [6]. As seen from Table 2, δ = 0.069 mm/s is the lowest value after the 772K treatment, even though nano-crystalline material could not be detected from the Mössbauer spectrum, as already discussed. Such a decrease in the value of δ implies an increase of the S-type electronic density inside the Fe nucleus [6]. Similarly, from the

temperature dependence of the quadrupole splitting (Δ_Q), additional changes of electronic density around the Fe atoms can also be inferred.

It can be observed from Table 2 that the values of Δ_Q also decrease in the temperature interval of 766 and 772K, suggesting the least distorted atomic symmetry and/or electronic density surrounding the Fe nuclei [6] after these thermal treatments. Thus, although the Mössbauer spectra do not detect nano-crystalline material between the 766 and 772K treatments, the Mössbauer parameters changed significantly within this temperature interval suggesting important micro-structural changes in the alloy prior to, or, at the start of its first crystallization process. These micro-structural changes are further studied by using PALS.

Conclusions

We studied the amorphous Fe-based alloy 2605S3A after heat treatment, by using several techniques. The positron annihilation process was used to measure clusters of 24 and 32 mono-vacancies in the amorphous and crystalline states of the alloy. We found that the clusters have 0.44 nm mean radii and a mean relative concentration of clusters between these states is equal to $C = 1.68 \times 10^{-8}$ atoms^{-1}. The glass and crystalline phase transitions temperatures (T_g and T_x) were measured with DSC. Our results suggested a relation between H_v minimum, associated with an increase of grain size and magnetic reorientation in the sample just before first phase transition. We applied the Mössbauer spectroscopy and Vickers micro-hardness measurements to detect nanometric changes in the sample. The significant changes in Mössbauer parameters, within temperature interval 766-772 K suggest important micro- and nanostructural changes in the alloy.

References

[1] Brener, A.; Riddell, G.E.: Nickel Plating on Steel by Chemical Reduction. J. of Research of the National Bureau of Standards, 37, 31 (1946).

[2]Cabral-Prieto, A.; Garcìa-Santibàñez, F.; Lòpez, A., Lòpez-Castañares, R.; Olea-Cardoso, O.: Vickers Microhardness and Hyperfine Magnetic Field Variations of Heat Treated Amorphous $Fe_{78}Si_9B_{13}$ Alloy Ribbons. Hyperfine Interactions **161**, 69 (2005).

[3] Allia, P.; Tiberto, P.; Baricco, M.: Vinai, F.: Improved ductility of nano-crystalline $Fe_{73.5}Nb_3Cu_1Si_{13.5}B_9$ obtained by direct-current joule heating, Appl. Phys. Lett., **83** (20), 2759 (1993).

[4] Bang, T.Y.; Lee R.Y.: Crystallization of the metallic glass $Fe_{78}Si_9B_{13}$, J. Mater. Sc. **26**, 4961 (1991)

[5] Linderoth, S.; Gonzalez, J. M.; Hidalgo, C.; Liniers, M.; Vincent, J. L. ;: Correlation between positron lifetime results and magnetic behavior upon relaxation and crystallization of an iron-based amorphous alloy. Solid State Commun. **65** (12), 1457(1988).

[6] Mössbauer Spectroscopy (1975), edited by U. Gonser, Springer-Verlag Berlin**,** Chapter 1,1-51.

[7] Particle Induced X-Ray Emission Analysis. Application to Analytical Problems, 1981. Edited by Zucker, A.: Oak Ridge National Laboratory.

[8] Brand R. A., User´s Guide of the Normos Mössbauer Fitting program, 1992. Distributed by Wissenschaftlich Elektronik GmbH.

[9] Xiangcheng Sun.; Cabral-Prieto, A.; Jose-Yacaman, M.; Reyes-Gasga, J.; Hernandez-Reyes, J. R.; Morales, A.; Sun, W.: Nano-crystallization behavior and magnetic properties of amorphous $Fe_{78}Si_9B_{13}$ ribbons, Phys. B 20921, 1 (2000).

[10] Li, J.M.; Quan,M.X.; Hu, Z.G.: Spectra investigation on Hall-Petch relationship in nano-crystalline $Fe_{78}Si_9B_{13}$ alloy, Appl. Phys. Lett. **69**, 1559 (1996).

[11] Murr, L.E.: A Form of Hall-Petch Law for the strength of Glassy Metals, Phys. Stat. Sol. (a) **61**, k101 (1980).

[12] S. Morimoto, S.; Ito, A.: Variation of magnetic anisotropy by heat treatment of amorphous alloy $(Co_{0.5}Fe_{0.5})_{74.5}Si_{13.5}B_{12}$ amorphous phase and precipitated crystalline phases, Phys. Rev. **B76**, 68 (1993).